Optical Second Harmonic Generation In Nanostructures With Inhomogeneous Magnetization

Irina A. Kolmychek[1,a], Victor L. Krutyanskiy[1,b], Tatiana Murzina[1,c] *,

Evgeniy A. Karashtin[2,d], Maxim V. Sapozhnikov[2,e] and Andrey A. Fraerman[2,f]

[1] Department of Physics, Moscow State University, 119991 Moscow, Russia

[2] Institute of microstructures, Nizhniy Novgorod, Russia
murzina@mail.ru

Abstract. The effects of inhomogeneous magnetization on optical second harmonic generation from magnetic nanostructures are studied. Cobalt triangular-shaped nanoparticles with vortex magnetization and magnetic trilayers that support the ferromagnetic phase formation are considered. We show that magnetic field dependencies of the SHG intensity for both types of structures reveal a number of distinct peculiarities associated with additional SHG mechanisms attributed to inhomogeneous magnetic state of the nanostructures.

Introduction

Magnetic nanostructures reveal rich variety of properties that originate from their design, composition and arrangement [1-3]. One of the attracting tasks here is the realisation of various types of magnetic ordering, which can find potential applications and are rare to be observed in natural media. Moreover, optical and especially nonlinear optical properties of such structures have attracted relatively low attention. At the same time, such studies can provide the development of a novel high-sensitive and relatively simple remote methods for the characterization of magnetic nanostructures.

In this paper we discuss our recent results on optical second harmonic generation (SHG) effects in noncentrosymmetric nanostructures with inhomogeneous magnetization, that are planar trilayer magnetic structures that support the antiferromagnetic state, and regular arrays of triangular-shaped cobalt nanostructures with vortex magnetization. We demonstrate that the usage of circular polarization of the probe beam allows to visualise the vortex magnetization and second-order magnetization-induced effects in trilayer magnetic films.

Experimental

2D lattice of uniformly oriented triangular-shaped cobalt dots with the side length of 700 nm on a glass substrate was fabricated by the electron-beam lithography and a lift-off technique [4]. The composed array is shown schematically in Fig.1, a. Regular arrangement of noncentrosymmetric magnetic particles results in their residual macroscopic vortex magnetization after the structure was magnetized along the sides of the Co dots, as is confirmed by the magnetic force microscopy (MFM) (Fig.1, b) and micromagnetic simulations (Fig. 1,c).

Trilayer magnetic structures of the composition $CoFe$(20 nm)/Al_2O_3(2nm)/$CoFe$(10 nm)Py (Fig. 3, a) were made by *rf* sputtering technique. The presence of a soft permalloy sublayer on the substrate decreases the coercive force of the $CoFe$ layer deposited on it, thus allowing for the formation of the antiferromagnetic state in the structure. Such a composition leads to a noncentrosymmetry in magnetization distribution. The schematic view of the structure is shown on the inset in Fig. 3.

The SHG experiments were performed using linearly or circularly polarized radiation of a Ti-sapphire laser operating at 800 nm wavelength and of the pulse width of 100 fs. The fundamental beam was focused into a spot of approximately 50 μm on the sample, the average intensity being about 40 mW, and the SHG at 400 nm was detected. The dependencies of the SHG intensity on the applied magnetic field, i.e. SHG magnetic hysteresis loops, were studied.

Results and Discussion
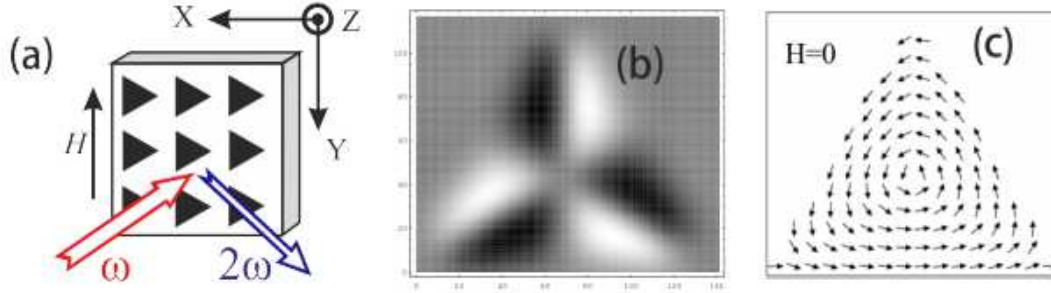   a) **Array of cobalt triangular nanodots**.

Fig. 1. (a) Scheme of the Co nanodots array; (b) MFM image of a single nanodot; (c) micromagnetic simulation of in-plane magnetization distribution in Co triangular dot.

A typical dependence of the linear magneto-optical Kerr effect (MOKE) from array of Co nanodots on the external longitudinal magnetic field is shown in Fig. 2, a. It reveals the vortex magnetization after the applying the saturating static magnetic field H, which appears as zero width of the MOKE hysteresis loop at H=0.

Magnetization-induced nonlinear-optical effects were studied in the geometry of the transversal magneto-optical Kerr effect for circularly polarized fundamental beam and specularly reflected p-polarized SHG. In order to reveal the vortex magnetization state, the SHG measurements were performed for the two different magnetization geometries. First, the structure was magnetized along the thiangles' height as is shown in Fig. 1,a, so that the vortices are randomly oriented in the structure. Second, the sample was magnetized along the side of the triangles, which leads to a macroscopic vortex magnetization of an array of nanodots, i.e. vorticity of all the triangular Co particles is the same. In the first case, the macroscopic magnetic vorticity is zero, that is why no difference between two branches of hysteresis loop at H=0 is detected (Fig. 2, b). Meanwhile, when the external field is applied along the triangles' side, a nonzero width of the SHG hysteresis loop at H=0 was obtained. This is consistent with our expectations that the two branches of the hysteresis loop correspond to different directions of macroscopic vortex magnetization (Fig. 2, c).

To explain the observed experimental results on SHG in inhomogeneous nanostructures with vortex magnetization, three contributions to the nonlinear polarization at the SHG wavelength should be considered: (i) crystallographic (*cr*), that is independent on the applied magnetic field; (ii) magnetic (*magn*) that is proportional to the average magnetization of the structure, that is *odd* in H and turns to zero at H=0; and (iii) the contribution induced by the macroscopic magnetic toroid moment (*tor*) [5] that evidently reaches its maxima at H = 0 and is zero for the saturating H values. The toroid moment changes its sign as the vorticity of magnetic particles is changed, so this contribution has the opposite signs for different branches of the SHG hysteresis loops.

$$I_{2\omega}(H) \propto |P(M)|^2 = |P^{cr} + P^{magn}(H) + P^{tor}(H)|^2 \tag{1}$$

The last two summands in (1) linearly depend on the magnetization (average or vortex) of the structure. An interference of these three contributions determines the observed SHG magnetic field dependencies. More detailed explanation of the observed phenomena is provided in [6].
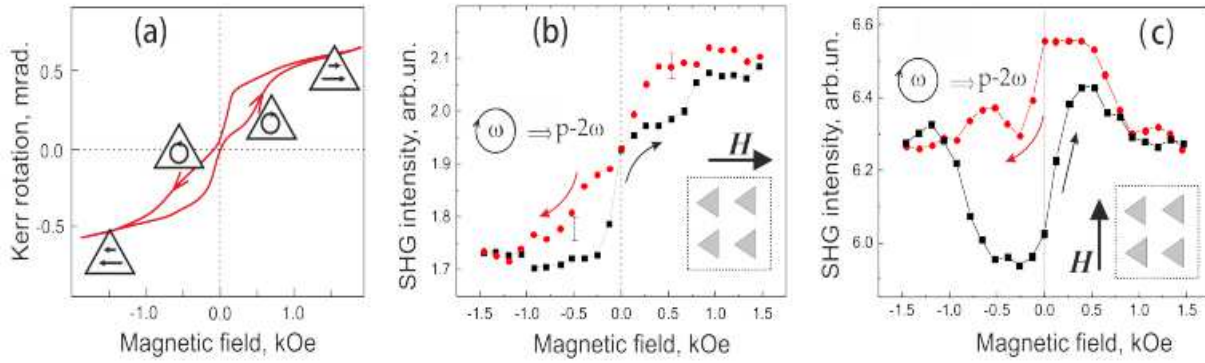
Fig. 2. (a) Dependence of MOKE on the applied magnetic field; Magnetic field dependencies of the SHG intensity for the (b) linearly and (c) circularly polarized fundamental radiation.

b) Trilayer structures

The dependence of the linear magneto-optical Kerr effect on the external magnetic field reveals clear "steps" that correspond to contributions of two magnetic layers to the registered MOKE signal, the coercive forces being H_{cI} = 93 Oe and H_{cII} = 14 Oe. Thus the nonlinear-optical response should also contain the contributions from the two magnetic layers. At the same time, there is a distinct difference between the linear and nonlinear-optical effects, as the SHG is forbidden in the bulk of centrosymmetric media such as metals and Al_2O_3(2nm) that compose the sample. As the inversion symmetry is broken at the interfaces, so the SHG response from each magnetic layer is formed by the nonlinear polarization at each of the two *interfaces*. We assume that the magnetic layers of the trilayer structure are homogeneous and isotropic, thus the borders of one layer uniformly depend on the applied magnetic field.

The dependence of the SHG intensity on the external magnetic field for the p-polarized fundamental beam is shown in Fig. 3, (b). The experimental data were approximated by the function: $I_{2\omega}(H) \propto \left(\left| \chi^{cr} + \chi_I^{odd} + \chi_{II}^{odd} \right| \right)^2$, where χ^{cr} is the crystallographic part; χ_i^{odd} is linear (i.e. first-order) in magnetization of the *i*-th magnetic layer (*I* or *II*), which was approximated as the following function of the external magnetic field $M_i \propto \arctan(H - H_{ci})$. It can be seen that the approximation curve is in a good agreement with the experimental data. We obtained the following relative values of the χ_i^{odd} susceptibilities $\left| \chi_I^{odd} / \chi^{cr} \right| \approx 0.11$, $\left| \chi_{II}^{odd} / \chi^{cr} \right| \approx 0.34$.

More interesting issues arise when the circularly polarized fundamental radiation was used; the corresponding experimental results are shown in (Fig. 3, (c)). It was obtained that at the angle of incidence of 25°, the interference of *odd* (i.e. first-order in *M*) effective nonlinear susceptibility components from the two layers gives nearly zero , so that the SHG magnetic contrast for the saturating magnetic fields is negligible. At the same time, *even* (i.e. second-order in *M*) contribution can be observed. The experimental SHG magnetic field dependence shown in Fig.3, (c) was approximated by the function $I_{2\omega}(H) \propto (| \chi^{cr} + \chi_I^{odd} + \chi_{II}^{odd} + \chi_I^{even} + \chi_{II}^{even} + \chi_{I,II}^{even} |)^2$, where χ_I^{even} and χ_{II}^{even} are proportional to $(M_I)^2$ and $(M_{II})^2$, correspondingly. In this expression we introduced the summand $\chi_{I,II}^{even}$ that is proportional to the scalar product $M_I M_{II}$. The symmetry of this SHG term corresponds to the exchange interaction of the two magnetic layers in the structure. The approximation of the experimental curves shows that this term should be necessary taken into account. Thus the following relative values of the susceptibility contributions were obtained: $\left| \chi_I^{odd} / \chi^{cr} \right| \approx 0.11$, $\left| \chi_I^{odd} / \chi^{cr} \right| \approx 0.16$, $\left| \chi_I^{even} / \chi^{cr} \right| \approx 0.10$, $\left| \chi_{II}^{even} / \chi^{cr} \right| \approx 0.10$, $\left| \chi_{I,II}^{even} / \chi^{cr} \right| \approx 0.23$. An important result here is that for the circularly polarized pump beam second-order in magnetization terms in the SHG field are observed, that are of the same order of magnitude as the first-order and the crystallographic terms.
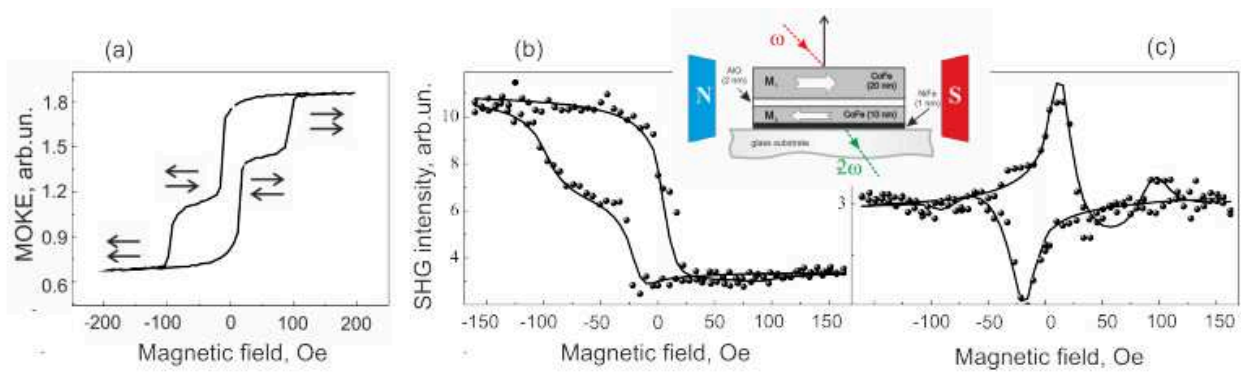
Fig. 3. (a) Schematic view of studied *CoFe/Al₂O₃/CoFe*-Py trilayer structure and of the transmission geometry of the experiment. Dependencies of the intensity of p-polarized SHG on the applied magnetic field for (b) linearly polarized and (c) circularly polarized fundamental radiation. Angle of incidence is 25 degrees.

Summary

Summing up, we investigated the effects of optical second harmonic in nanostructures with non-centrosymmetric and inhomogeneous distribution of magnetization. Namely, regular arrays of triangular Co nanoparticles with vortex magnetization and a planar trilayer films are studied. We demonstrate that when using the circularly polarized pump beam, macroscopic magnetic toroid moment for vortex nanoparticles and second-order in magnetization components of the SHG field can be evaluated.

References

[1] Y. Z.Wu, R. Vollmer, H. Regensburger,X. F. Jin, J. Kirschner, "Magnetization-induced second harmonic generation from the Ni/Cu interface in mutlilayers on Cu (001)", Phys. Rev. B 63 (2000) 054401.

[2] A. Granovsky, M. Kuzmichov, J.P. Clerc, M. Inoue, „Effective-medium theory for nonlinear magneto-optics in magnetic granular alloys: cubic nonlinearity", J. Magn. Magn. Mater. 258-259 (2003) 103.

[3] V.K. Valev, A. Kirilyuk, F. Dalla Longa, J.T. Kohlhepp, B. Koopmans, Th. Rasing, "Observation of periodic oscillations in magnetization-induced second harmonic generation at the Mn/Co interface", Phys.Rev. B 75 (2007) 012401.

[4] A. A. Fraerman, S. A. Gusev, L. A. Mazo, I. M. Nefedov, Y. N. Nozdrin, I. R. Karetnikova,M. V. Sapozhnikov, I. A. Shereshevskii, L. V. Sukhodoev, "Rectangular lattices of permalloy nanoparticles: Interplay of single-particle magnetization distribution and interparticle interaction", Phys. Rev. B 65 (2002) 064424.

[5] A.A. Gorbatsevich, Y.V. Kopaev, Ferroelectrics 161 (1994) 321334.
[6] V. L. Krutyanskiy, I. A. Kolmychek, B. A. Gribkov, E. A. Karashtin, E. V. Skorohodov, T. V. Murzina, "Second harmonic generation in magnetic nanoparticles with vortex magnetic state", Phys. Rev. B 88 (2013) 094424.

Achievements in Magnetism

Optical Second Harmonic Generation in Nanostructures with Inhomogeneous Magnetization

DOI References

[1] Y. Z. Wu, R. Vollmer, H. Regensburger,X. F. Jin, J. Kirschner, Magnetization-induced second harmonic generation from the Ni/Cu interface in mutlilayers on Cu (001), Phys. Rev. B 63 (2000) 054401.
http://dx.doi.org/10.1103/PhysRevB.63.054401

[2] A. Granovsky, M. Kuzmichov, J.P. Clerc, M. Inoue, Effective-medium theory for nonlinear magneto-optics in magnetic granular alloys: cubic nonlinearity, J. Magn. Magn. Mater. 258-259 (2003) 103.
http://dx.doi.org/10.1016/S0304-8853(02)01078-8

[3] V.K. Valev, A. Kirilyuk, F. Dalla Longa, J.T. Kohlhepp, B. Koopmans, Th. Rasing, Observation of periodic oscillations in magnetization-induced second harmonic generation at the Mn/Co interface, Phys. Rev. B 75 (2007) 012401.
http://dx.doi.org/10.1103/PhysRevB.75.012401

[4] A. A. Fraerman, S. A. Gusev, L. A. Mazo, I. M. Nefedov, Y. N. Nozdrin, I. R. Karetnikova,M. V. Sapozhnikov, I. A. Shereshevskii, L. V. Sukhodoev, Rectangular lattices of permalloy nanoparticles: Interplay of single-particle magnetization distribution and interparticle interaction, Phys. Rev. B 65 (2002).
http://dx.doi.org/10.1103/physrevb.65.064424

[6] V. L. Krutyanskiy, I. A. Kolmychek, B. A. Gribkov, E. A. Karashtin, E. V. Skorohodov, T. V. Murzina, Second harmonic generation in magnetic nanoparticles with vortex magnetic state, Phys. Rev. B 88 (2013) 094424.
http://dx.doi.org/10.1103/PhysRevB.88.094424